The "Independence Principle" in the Processes of Water Transport

Julio A. Hernández* and Jorge Fischbarg‡

*Sección Biofísica, Facultad de Ciencias, Universidad de la República, 11200 Montevideo, Uruguay, and ‡Departments of Physiology and Cellular Biophysics, and Ophthalmology, College of Physicians and Surgeons, Columbia University, New York, New York 10032 USA

ABSTRACT The processes of membrane transport exhibiting permeability coefficients depending on the species activities do not obey the "independence principle" and are assumed to take place by a mechanism of discrete nature, analyzable by a kinetic formalism. In this article, we study the dependence of the osmotice permeability coefficient on the water activities, from the steady-state analysis of a kinetic model of single-file water transport that simultaneously incorporates the vacancy-mediated and "knock-on" mechanisms into the state diagram. In particular, we study the relation between the near-equilibrium osmotic permeability (P_e) and the equilibrium water activity of the compartments (w). The analysis and numerical calculations performed for a simple case of the model show that, for values of the parameters consistent with experimental data, P_e exhibits only a small variation with w within the physiological range in the majority of the situations considered here. It is not possible to predict, from the study of these simple models, whether more complicated kinetic diagrams of water transport may be characterized by permeability coefficients with a more evident dependence on the water activities. Nevertheless, the results obtained here suggest that, for the case of physiological water pores, the analysis of the kinetic dependence of the permeability coefficients on the water activities may not yield evidence pointing to a discrete nature for the transport process.

INTRODUCTION

The molecular nature of the mechanisms of water and solute transport through biological membrane pores remains unknown. Many studies of the theory of transport analyze a single-file model, one of the simplest mechanisms of pore transport. This mechanism has been proposed for diverse membrane systems; the gramicidin A pore constitutes the classical example (Finkelstein, 1987; Hille, 1992). To describe single-file water transport, two types of molecular models have been developed: continuum and discrete. Continuum models have included dynamical analysis under near-equilibrium conditions (Levitt, 1974; Finkelstein and Rosenberg, 1979) and linear thermodynamic analysis (Levitt, 1984). Both types of studies implicitly assume a "knock-on" mechanism (Hodgkin and Keynes, 1955). Discrete processes at the molecular level are usually represented by means of kinetic models. Kinetic models have been diversely employed to interpret properties in one-ion and multi-ion pores (see Hille, 1992), and in the special case of saturation conditions in ionic (Kohler and Heckmann, 1979, 1980; Schumaker and MacKinnon, 1990) and water (Hernández and Fischbarg, 1992) single-file pores.

The expressions for the permeability coefficients of the transported species reflect the basic difference between continuum and discrete mechanisms. Although in continuum models the permeability coefficients usually depend on a single system parameter (e.g., for the case of water, a viscosity coefficient) and are independent of the activities of the same and of different species, in discrete models they generally depend on more than one system parameter (e.g., several first-order rate constants) and are functions of the species activities. Thus, the "independence principle" applies to the former but not to the latter case (Schultz, 1980).

In a previous article (Hernández and Fischbarg, 1992), we derived explicit expressions for the osmotic and diffusive permeability coefficients of water from the analysis of a kinetic model of single-file water transport. Two different cases were considered: one-vacancy and "knock-on" (no-vacancy, or saturation) mechanisms. As expected (see above), the expressions derived there for the permeability coefficients in the case of vacancy-mediated transport are functions of the water activities. Instead, for the "knock-on" mechanism, the coefficients were shown to comply with the "independence principle."

In this article, we explore the dependence of the osmotic permeability coefficient of a kinetic model for water transport that includes simultaneously in its diagram both vacancy and "knock-on" mechanisms. We term this a "complete" kinetic model of water transport. We seek to determine whether for physiological values of the water activities and osmotic permeability coefficients, such complete kinetic model may conform to the "independence principle." With this purpose, we analyze here a complete kinetic model of single-file water transport.

In the first part, we discuss the complexity inherent to the study of this type of "complete" kinetic models of single-file transport, and we analyze the limiting behaviors of these models. In the second part, we study the dependence of the near-equilibrium osmotic permeability coefficient P_e on the equilibrium water activity. For illustration, we show numerical examples of this dependence for a particular simple case.

"COMPLETE" KINETIC MODELS OF SINGLE-FILE TRANSPORT

In Fig. 1 we show the simplified state diagram for a "complete" kinetic description of water transport through a

Received for publication 13 December 1993 and in final form 1 June 1994.

Address reprint requests to Dr. Jorge Fischbarg, Departments of Physiology Cellular Biophysics and Ophthalmology, College of Physicians and Surgeons, Columbia University, New York, NY 10032. Tel.: 212-305-9092; Fax: 212-305-2461; E-mail: fischbarg@cuccfa.ccc.columbia.edu.

0006-3495/94/10/1464/09 $2.00

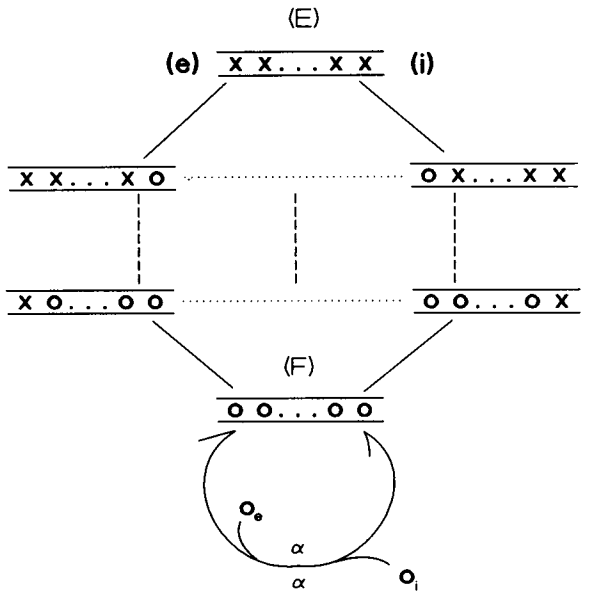

FIGURE 1 A simplified kinetic diagram showing vacancy-mediated and "knock-on" mechanisms of transport of a single species through a one-conformational single-file pore, between compartments "e" and "i". (X) Vacancies; (O) positions occupied by molecules. "E" and "F" are the completely empty and occupied states, respectively. In the vacancy portion, the diagram only shows the limiting cycles corresponding to single-occupancy and single-vacancy transport. In each cycle, the punctuated line represents a linear sequence of transitions. The network of states and transitions connecting these cycles is suggested by the broken lines. For an example showing this portion in detail, see Fig. 2. See also text for further details.

one-conformational single-file pore with a maximum of n occupancy sites in the file. The diagram includes the vacancy-mediated region (from one to n vacancies) and the single loop representing the "knock-on" mechanism (Hernández and Fischbarg, 1992). For simplicity, the vacancy region only shows the cycles for the single-occupancy and the single-vacancy limiting behaviors. States "E" and "F" in Fig. 1 are the states having n vacancies and no vacancies, respectively. Hence, the "knock-on" loop implies a transition between state "F" and itself. The detailed balance restriction requires that the same rate constant ("α") will govern the frequency of transition in either direction. Here and elsewhere, we analyze the model of Fig. 1 by means of the graphic algorithm originated by King and Altman (1956) and modified by Hill (1977).

We assume that water traverses a membrane unit area through N identical pores that behave as in the model of Fig. 1. Hence, the osmotic permeability coefficient P_w of the membrane is given by

$$P_w = \left(\frac{N}{\sum}\right)\left(S_i + \sum_F \alpha\right). \quad (1)$$

In Eq. 1, S_i represents a sum, taken over all the cycles of the vacancy portion that determine net water transport, of terms of the form $\sum_i \pi_i$. For a particular cycle i, $\sum_i$ is the sum of all the appendages to the cycle and π_i is, from the detailed balance restriction, the product of all the rate constants in any of the two directions of the cycle. The term $\sum_F$ is the sum of all the directional diagrams that feed into state "F." The denominator $\sum$ is the sum of all the directional diagrams of all the states of the model. Because the "knock-on" transition constitutes a cycle, it does not contribute with terms to $\sum$. Hence, $\sum$ is given by the same expression, both for the "complete" model including the "knock-on" transition (Fig. 1) and for the model corresponding to the vacancy portion only. For the same reason, $\sum_F$ also equals the corresponding term emerging from the vacancy portion of the diagram only.

The limiting behaviors of P_w (Eq. 1) as a function of the water activities in the two compartments (w_i and w_e) can be analyzed in general terms:

a) When $(w_i, w_e) \to 0$, P_w approaches the single-occupancy cycle limit, i.e., $P_w \to N\,\pi/\Omega_{so}$. Here π is the product of all the rate constants of the single-occupancy cycle in any of the two directions and Ω_{so} is the sum of all the directional diagrams of all the states corresponding to the single-occupancy cycle only.

b) When $(w_i, w_e) \to \infty$, $\sum \to \sum_F$, because $\sum_F$ contains the terms of the higher order in the water activities. Correspondingly, S_i contains terms of lower order in the water activities and, therefore, in this limit, $NS_i/\sum \to 0$, because it is characteristic of a saturation process. Hence, if α is not negligible, $P_w \to N\alpha$, the osmotic permeability coefficient of a process mediated exclusively by a "knock-on" mechanism (Hernández and Fischbarg, 1992).

In Fig. 2 we show the state diagram of vacancy-mediated transport of a single species through a single-file pore, for the case that $n = 3$. A similar model has been employed, for instance, to interpret some basic general properties of ionic channels (Hille, 1975). The steady-state kinetic analysis of this type of model can be performed employing standard methods, like matrix inversion or diagrammatic techniques (Hill, 1977). The application of the method developed by Hill (1977) shows the complexity inherent in the analysis of the

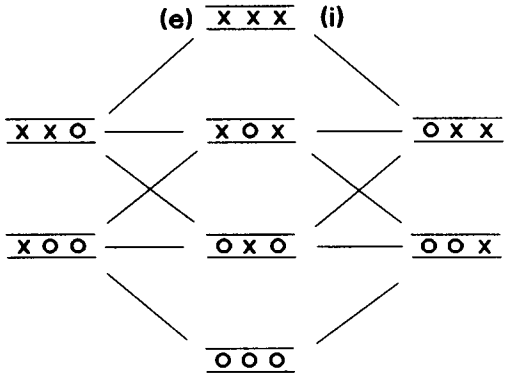

FIGURE 2 Kinetic model of vacancy-mediated transport of a single species through a one-conformational single-file pore containing three binding positions for the transported molecules. (X) Vacancies; (O) positions occupied by molecules. Compartment "e" is assumed to be on the left side, compartment "i" is on the right side of the pore. The solid lines represent actual transitions between the diagram states. The binding of molecules at the corresponding steps is not explicitly shown. See text for further details.

model of Fig. 2. Indeed, this model has 8 pore states, gives rise to 22 cycle diagrams, and contains more than 1000 directional diagrams, all of which make the derivation of explicit analytical expressions rather impractical. The analysis of the general case of n positions would certainly be even much more involved.

Kinetic analyses of single-file transport have been performed for the limiting case of one-vacancy pores (Kohler and Heckmann, 1979, 1980; Schumaker and MacKinnon, 1990; Hernández and Fischbarg, 1992). Explicit analytical studies of the kinetic model of vacancy-mediated single-file transport have already been done for the particular case that $n = 2$, for a pore having from 0 to 2 vacancies, and in the presence of one or two ionic ligands (Heckmann, 1965a, b, 1968; Urban and Hladky, 1979; Urban et al., 1980). These authors employed the algebraic procedure of successive elimination of unknowns to solve the velocity equations in steady state. For the purpose of our work, some basic ideas can be extracted from the analysis of the simple case $n = 2$. In the rest of this section, we show the basic properties of the analytical expressions for the "complete" model when $n = 2$ (Fig. 3, and Appendix). We use the diagrammatic technique developed by Hill (1977).

From Eq. A2, the permeability coefficient P_w for the model of Fig. 3 is

$$P_w = \left(\frac{N}{\sum}\right)[\pi(\sum_1 + \sum_2) + \sum_F \alpha], \tag{2}$$

where π, $\sum$, $\sum_1$, and $\sum_2$ are defined in the Appendix, and where N, $\sum_F$, and α have the same meanings as in Eq.1. As can be seen, P_w depends on the activities w_e and w_i and, therefore, does not obey the "independence principle" (Schultz, 1980). Notice that if α is negligible, P_w corresponds to the permeability coefficient of the vacancy model (see Eq. A2).

Under the condition

$$\begin{aligned} b_e w_e + b_i w_i \gg r_e + r_i \quad \text{and} \quad r_e r_i, \\ r_e^2 \quad \text{and} \quad r_i^2 \quad \text{negligible}, \end{aligned} \tag{3}$$

the term $\sum$ becomes

$$\sum = \Omega_2 \sum_2, \tag{4}$$

where Ω_2 is defined in the Appendix. Also from condition (3), we obtain

$$\sum_1 + \sum_2 = \sum_2. \tag{5}$$

From (4) and (5), Eq. 1 becomes

$$P_w = N\left[\left(\frac{\pi}{\Omega_2}\right) + \left(\frac{\sum_F \alpha}{\sum}\right)\right]. \tag{6}$$

If α is negligible, Eq. 6 becomes Eq. A11. Therefore, under condition (3) and for a negligible contribution of the "knock-on" mechanism, the kinetic properties of the model in Fig. 3 *A* are given by the single cycle 2 (Fig. 3 *B*). Cycle 2 represents the particular case $n = 2$ of the general one-vacancy single-file pore model, studied elsewhere as a model of multi-occupancy ionic or water pores (Kohler and Heckmann, 1979, 1980; Schumaker and MacKinnon, 1990; Hernández and Fischbarg, 1992).

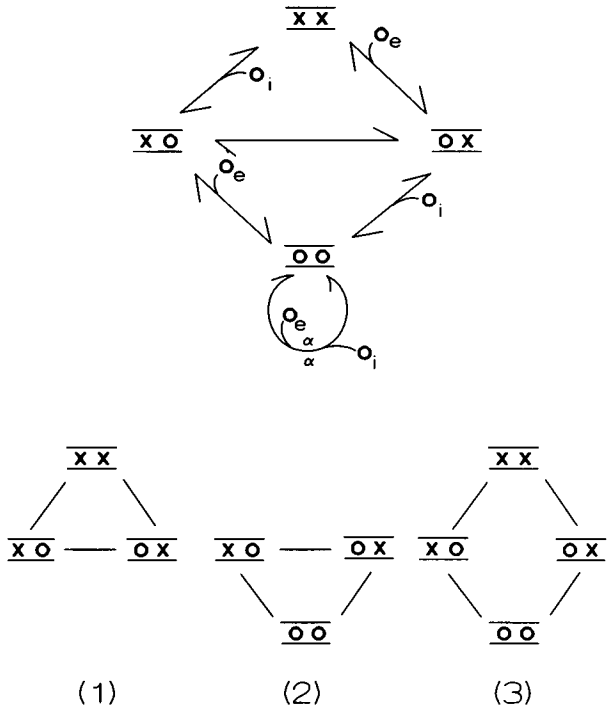

FIGURE 3 Kinetic model of transport of a single species through a single-file pore containing two binding positions for the transported molecules, including both the vacancy and "knock-on" mechanisms. Xs, open circles, and compartments are as in Fig. 2. Positions inside the pore are numbered "1" and "2" in the *e* to *i* direction. (*A*) The complete state diagram. The solid lines represent actual transitions between states. See text for the definition of the rate constants corresponding to the particular transitions. (*B*) The three cycles arising from the vacancy portion of the kinetic model of *A*.

Under the condition

$$\begin{aligned} r_e + r_i \gg b_e w_e + b_i w_i \quad \text{and} \quad b_e w_e b_i w_i, \\ (b_e w_e)^2 \quad \text{and} \quad (b_i w_i)^2 \quad \text{negligible}, \end{aligned} \tag{7}$$

the term $\sum$ becomes

$$\sum = \Omega_1 \sum_1, \tag{8}$$

where Ω_1 is defined in the Appendix. Also from condition (7) we obtain, in this case,

$$\sum_1 + \sum_2 = \sum_1. \tag{9}$$

Under condition (7), $\sum_F$ becomes negligible. Therefore, from (8) and (9), Eq. 2 now becomes

$$P_w = N\pi/\Omega_1, \tag{10}$$

which is identical with Eq. A10. Therefore, under condition (7) the kinetic properties of the model in Fig. 3 *A* are given by the single cycle 1 (Fig. 3 *B*). Cycle 1 represents the particular case $n = 2$ of the general single-occupancy pore model, diversely employed to describe ionic transport (for a review and references, see Hille, 1992).

For the case of a negligible contribution of the "knock-on" mechanism, conditions (3) and (7) therefore determine the limiting behaviors corresponding to single-vacancy and single-occupancy transport, respectively. It is possible that these basic conditions can be generalized to an arbitrary n. This is suggested by the general features and symmetry of the diagrams (see Figs. 2 and 3) and by some results on the asymptotic behavior of the multi-vacancy model under near-saturation conditions (Kohler and Heckmann, 1979, 1980). If α is not negligible, the one-vacancy mechanism does not represent a good approximation to describe transport under near-saturation conditions. In this latter case, and for the simple example analyzed here, α must appear in the treatment, and P_w would be given by Eq. 6, which expresses the simultaneous contribution of the one-vacancy and "knock-on" mechanisms. In other words, for near-saturating water activities, water transport through one-conformational single-file pores would take place by a mixture of discrete (one vacancy-mediated) and continuum-like (e.g., "knock-on") regimes.

OSMOTIC PERMEABILITY COEFFICIENT: DEPENDENCE ON THE WATER ACTIVITIES

For the case of one-conformational narrow pores, a plausible description of the transport process is provided by Fig. 1, and the permeability coefficient correspondingly is given by Eq. 1. As mentioned above, if α is negligible, the permeability coefficient given by an expression of the type of Eq. 1 corresponds to a system exhibiting saturation kinetics, typical of a process that does not obey the "independence principle" (Schultz, 1980). Under this condition, the permeability coefficient should decrease with the species activities, as emerges from inspection of Eqs. 1 and 2. For water, this would imply a "non-Newtonian" type of behavior, because the osmotic permeability coefficient would then depend on the water activities (or the equivalent osmotic or hydrostatic pressures). Conversely, for water transport to comply with the independence principle constitutes the microscopical counterpart of the "Newtonian" behavior of classical hydrodynamics.

We first analyze in this section the relation between P_w and the equilibrium activity of water (w) for the simple case under consideration (Fig. 3) and then show some numerical examples. As also commented above, the complexity of the diagrams representing larger pores restricts our study to the case that $n = 2$. Therefore, the contents of this section should mainly be considered as an example of a possible approach to the problem, and as an illustration of the behavior that actual biological water pores may exhibit.

To further simplify the study, we assume that

$$b_e = b_i = b; \quad r_e = r_i = r; \quad \text{and} \quad k_{12} = k_{21} = k. \tag{11}$$

Condition (11) corresponds to a "symmetrical" pore. Near equilibrium, we assume that $w_e = w_i = w$. In this case, and under condition (11), Eq. 2 becomes

$$P_e = (P_w)_{eq} = P_v + P_{ko}, \tag{12}$$

where P_v corresponds to the contribution of the vacancy portion to the overall near-equilibrium permeability coefficient P_e, and is given by

$$P_v = \frac{Nkrb}{(r + bw)(r + bw + 2k)}, \tag{13}$$

and where P_{ko}, provided by the "knock-on" mechanism, is given by

$$P_{ko} = \frac{Nb^2w^2\alpha}{(r + bw)^2}. \tag{14}$$

We now ask ourselves whether the determination of P_e at two "extreme" experimental values of w, w_1 and w_2, could put in evidence a noticeable difference between the corresponding permeability coefficients. For this purpose, we define

$$\Delta w = w_2 - w_1, \tag{15}$$

where w_1 and w_2 are two particular values of w, such that $w_2 > w_1$. Hence, from Eqs. 12–14, the difference between the corresponding near-equilibrium permeability coefficients, ΔP_e, is given by

$$\Delta P_e = P_e(w_2) - P_e(w_1) = \Delta P_v + \Delta P_{ko}, \tag{16}$$

where, for this particular example (condition (11),

$$\Delta P_v = Nbrk\left\{\frac{1}{(r + bw_2)(r + bw_2 + 2k)} - \frac{1}{(r + bw_1)(r + bw_1 + 2k)}\right\}, \tag{17}$$

and

$$\Delta P_{ko} = Nb^2\alpha\left[\frac{w_2^2}{(r + bw_2)^2} - \frac{w_1^2}{(r + bw_1)^2}\right]. \tag{18}$$

From Eqs. 15–18, we can express ΔP_v, ΔP_{ko} and, therefore, ΔP_e as functions of Δw, w_1, and the parameters. We now consider two situations.

i) α negligible.

In this case, ΔP_e approximately corresponds to ΔP_v that, for the example under consideration, is given by Eq. 17. From this expression and from definition (15), we see that ΔP_v is of the form

$$\Delta P_v = -\frac{\Delta w(L_0 + L_1w_1)}{M_0 + M_1w_1 + M_2w_1^2 + M_3w_1^3 + M_4w_1^4}, \tag{19}$$

where the Ls and the Ms are positive functions of Δw and of the parameters.

When

$$w_1 \to 0, \qquad \Delta P_v \to -\frac{\Delta wL_0}{M_0}, \tag{20}$$

where

$$L_0 = Nbkr[2b(r + k) + b^2\Delta w], \tag{21}$$

and

$$M_0 = r(2k + r) \times \{r(2k + r) + \Delta w[2b(r + k) + b^2\Delta w]\}. \tag{22}$$

When

$$w_1 \to \infty, \qquad \Delta P_v \to 0. \tag{23}$$

Hence, the limits (20) and (23) are characteristic of a transport process exhibiting saturation kinetics. Because from Eq.19 the absolute value of ΔP_v (ΔP_e in this case) decreases monotonously with w_1, the maximum absolute value of ΔP_v is achieved in the limit given by (20). From a biological point of view, this limit constitutes an unrealistical condition. In the vast majority of the situations, physiological water activities correspond to the saturation region. Therefore, a transport model of the type of Fig. 3 is likely to exhibit small (if not negligible) variations of the permeability coefficient as a function of the water activities, even in the case that the basic mechanism of transport is mostly of discrete nature.

ii) α not negligible.

In this case, the contribution of the term ΔP_{ko} to the overall difference ΔP_e (Eq. 16) should be considered. From Eqs. 15 and 18, we see that the expression for ΔP_{ko} is of the form

$$\Delta P_{ko} = \frac{\Delta w(J_0 + J_1 w_1 + J_2 w_1^2)}{K_0 + K_1 w_1 + K_2 w_1^2 + K_3 w_1^3 + K_4 w_1^4}, \tag{24}$$

where the Js and the Ks are positive functions of Δw and of the parameters. Hence, Eq. 24 always represents a positive function.

When

$$w_1 \to 0, \qquad \Delta P_{ko} \to \frac{\Delta w\, J_0}{K_0}, \tag{25}$$

where

$$J_0 = N\alpha b^2 r^2 \Delta w, \tag{26}$$

and

$$K_0 = r^2[r^2 + \Delta w(2br + b^2\Delta w)], \tag{27}$$

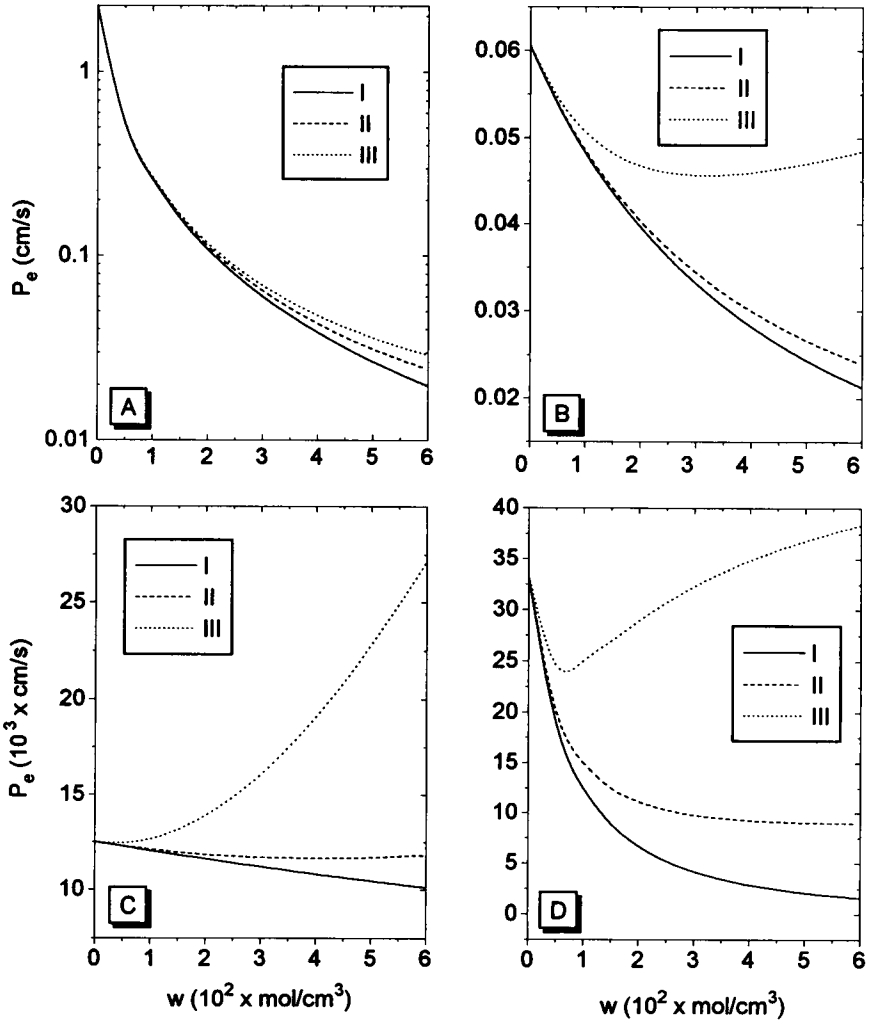

FIGURE 4 Plots of P_e as a function of w, using Eqs. 12–14, for different sets of values of the rate constants b ($cm^3\ mol^{-1}\ s^{-1}$), k (s^{-1}), r (s^{-1}), and α ($cm^3\ mol^{-1}\ s^{-1}$). For all the curves, $N = 10^{-12}$ mol/cm^2. (*A*) $b = 5 \times 10^{12}$; $k = 5 \times 10^{10}$; $r = 10^{10}$; α = 0(I), 5×10^9(II), 10^{10}(III). (*B*) $b = 10^{10}/0.055$; $k = r = 10^{10}$; α = 0(I), 10^{10}(II), 10^{11}(III). (*C*) $b = 5 \times 10^{10}$; $k = 10^{10}$; $r = 2 \times 10^{10}$; α = 0(I), 10^{11}(II), 10^{12}(III). (*D*) $b = 10^{11}$; $k = 10^9$; $r = 10^9$; α = 0(I), 10^{10}(II), 5×10^{10}(III). See text for comments.

If Δw is sufficiently small, we can neglect terms in $(\Delta w)^2$. In this case, the contribution of the "knock-on" term ((25)) to the limit $\Delta P_e(w_1 \to 0)$ is negligible, and this limit, therefore, is given by (20).

When

$$w_1 \to \infty, \qquad \Delta P_{ko} \to 0. \tag{28}$$

Similarly to the absolute value of ΔP_v (Eq. 19), Eq. 24 also decreases monotonously with w_1. Therefore, considering the limit given by (28), determinations of ΔP_e performed at saturating ws are not likely to put in evidence significant differences in the permeability coefficients, independently of whether α is negligible or not.

We employ the equations derived in the first part of this section to perform some numerical calculations. Typical values of pore-mediated osmotic permeability of the most water-permeable cells studied are of the order of 10^{-2} cm/s (House, 1974; Finkelstein, 1987; Verkman, 1992). We also assume, for the calculations, that N is 10^{-12} mol/cm^2, corresponding approximately to 6.10^{11} pores per cm^2, a plausible value for the number of water channels in the erythrocyte membrane (Denker et al., 1988; Preston et al., 1992). Assuming these values, the water permeability per pore would be of the order of 10^{-14} cm^3/s, the approximate value predicted for the pore formed by gramicidin A (Finkelstein, 1987). To perform the calculations that follow, we consider that the amount of water transported through the lipid bilayer is negligible. The values assumed for the rate constants are arbitrary. The only criteria for their choice is the plausibility, from a physiological point of view, of the values obtained for the permeability coefficients as functions of the equilibrium water activity.

Figs. 4 and 5 show calculations corresponding to the "complete" model of Fig. 3, and for a wide range of values of the equilibrium water activity. In Figs. 6 and 7 we restricted the study to the behavior of the vacancy portion of the model only, and for a narrower, closer to physiological, range of the water activities.

Fig. 4 shows the dependence of P_e on the equilibrium water activity w, as given by Eqs. 12–14, for different sets of values of the rate constants. As can be seen, for the physiological values of P_e (about 10^{-2} cm/s) and of w (about 0.055 mol/cm^3), curves I, II, and III of Fig. 4 *A*, and curves I and II of Fig. 4 *B–D*, correspond to the saturation zone. In

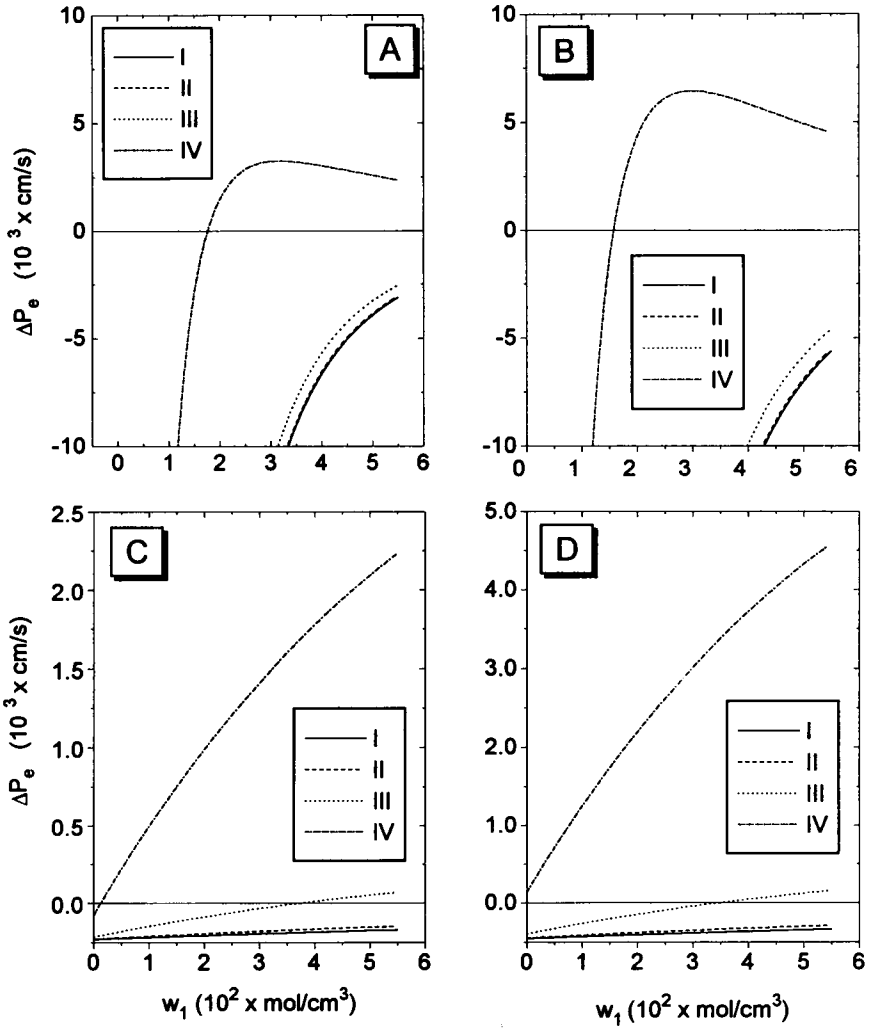

FIGURE 5 Plots of ΔP_e as a function of w_1, using Eqs. 15–18, for different sets of values of the rate constants b (cm^3 mol^{-1} s^{-1}), k (s^{-1}), r (s^{-1}) and α (cm^3 mol^{-1} s^{-1}), and of Δw (mol/cm^3). (*A* and *B*) $b = 5 \times 10^{12}$, $k = 5 \times 10^{10}$, $r = 10^{10}$. (*C* and *D*) $b = 5 \times 10^{10}$, $k = 10^{10}$, $r = 2 \times 10^{10}$. (*A* and *C*) $\Delta w = 0.005$. (*B* and *D*) $\Delta w = 0.01$. For every plot $\alpha = 0$(I), 10^{10}(II), 10^{11}(III), 10^{12}(IV). See text for comments.

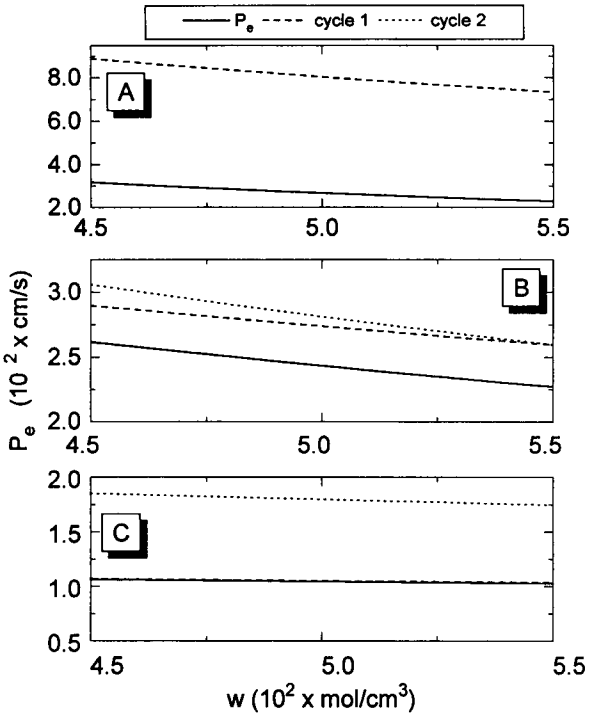

FIGURE 6 Plots of P_e as a function of w using Eq. 13, for different sets of values of the rate constants b (cm^3 mol^{-1} s^{-1}), k (s^{-1}), and r (s^{-1}). Plots of Eqs. A10 and A11 under condition 11 and for equilibrium activities of w, corresponding to the permeability coefficients of the single cycles 1 and 2, respectively, are also included (curves 1 and 2, respectively). For all the curves $N = 10^{-12}$ mol/cm^2. (A) $b = 5 \times 10^{12}$, $k = 5 \times 10^{10}$, $r = 10^{10}$; (6) $b = 10^{10}/0.055$, $k = r = 10^{10}$; (6) $b = 5 \times 10^{10}$, $k = 10^{10}$, $r = 2 \times 10^{10}$. See text for comments.

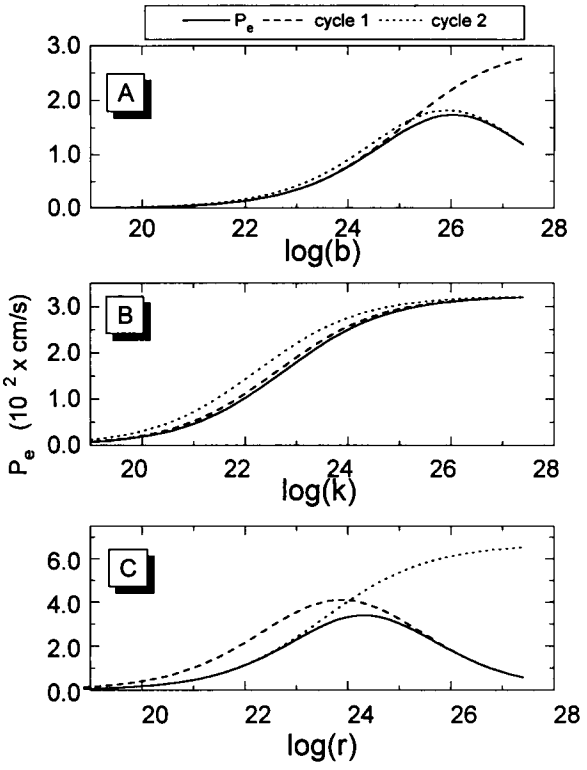

FIGURE 7 Plots of P_e as a function of the different rate constants b (cm^3 mol^{-1} s^{-1}), k (s^{-1}), and r (s^{-1}), using Eq. 13. For all the curves, $N = 10^{-12}$ mol/cm^2 and $w = 0.055$ mol/cm^3. Plots of the permeability coefficients corresponding to cycles 1 and 2 are also included, as in Fig. 6. (A) $k = 10^{10}$, $r = 5 \times 10^9$; (B) $b = 10^{11}$, $r = 10^{10}$; (C) $b = 5 \times 10^{11}$, $k = 10^{10}$. See text for comment.

curve III of Fig. 4 *B–D*, the combination of values assigned to the rate constants yield "unphysiological," namely too large, values of P_e in the physiological range of values of w.

Fig. 5 shows the dependence of ΔP_e on the equilibrium water activity w_1, as given by Eqs. 16–18, for different sets of values of the rate constants and of Δw. Fig. 5, *A* and *B* on one side, and Fig. 5, *C* and *D* on the other, show plots performed using the same set of vales of the rate constants, respectively. They only differ between them in the value employed for Δw. As can be seen, in an intermediate portion of the curves, ΔP_e increases with Δw. To be noted, the absolute value of the difference ΔP_e remains very small, even in the cases closest to physiological behavior. Curve IV of Fig. 5, *C* and *D*, showing a portion of the function notoriously increasing with w, corresponds to the "unphysiological" values of the rate constants that determine curve III of Fig. 4 *C*.

Fig. 6 shows the dependence of P_e on the near-equilibrium water activity w for different sets of values of the rate constants b, k, and r, and for a negligible contribution of the "knock-on" mechanism (e.g., $\alpha = 0$). For each set of constants, we plot the permeability coefficients corresponding to the complete model (P_e) as well as the permeability coefficients corresponding to the limiting cycles 1 and 2 (curves 1 and 2, respectively). This allows us to evaluate the accuracy of the single cycle approximations for the range of w considered. As can be seen, the model is able to display both non-Newtonian (Fig. 6, *A* and *B*) and quasi-Newtonian behavior (Fig. 6 *C*), depending on the particular values of the rate constants. However, considering the very large range of water activities studied, the observed variation of the permeability coefficients is very small, even in the most extreme cases depicted in Fig. 6, *A* and *B*. Superpositions occur between curve 2 and P_e in Fig. 6 *A* and between curve 1 and P_e in Fig. 6 *C*. In the former case, condition (3) applies, whereas condition (7) applies in the latter example.

Fig. 7 shows the dependence of P_e on each of the rate constants, for the cases of the vacancy region, and of the single cycles 1 and 2. As may be deduced from an analysis of Eq. 13, P_e increases and then decreases around a maximum, as a function of both r and b (Fig. 7, *A* and *C*, respectively). Therefore, in both of these cases, P_e is not single-valued, because similar values of P_e can be obtained for two different values of the corresponding rate constant. Also, P_e exhibits "saturation kinetics" as a function of k (Fig. 7 *B*). In this vacancy model, the resulting functions of P_e approximately correspond to a transition between the regimes determined by each one of the limiting cycles.

DISCUSSION

Water channel proteins plus some transporters and channels have been demonstrated to constitute sites of water transport across cell membranes (nicotinic acetylcholine receptor (Dani, 1989); facilitative glucose transporters (Fischbarg et al., 1990; Zhang et al., 1991); CHIP28 water channel (Preston et al., 1992); Cystic Fibrosis transmembrane conductance regulator (Hasegawa et al., 1992)). Many of them may operate via narrow inner channels by means of a single-file mechanism. The model in Fig. 1 represents the most general description of the processes of transport taking place in one-conformational single-file pores, because it includes a variety of behaviors ranging from the single-occupancy to the fully saturated "knock-on" mechanisms. Thus, Eq. 1 expresses the permeability coefficient resulting from a coexistence of different regimes and allows one to derive particular limiting cases.

The results obtained in the first part of the present work show that, under near-saturating water activities, the permeability coefficients derived from the single-file water transport model reflect practically only the properties of the one-vacancy and full saturation (e.g., "knock-on") modes. This analytical result agrees with the evidence that emerges from molecular dynamics simulations of gramicidin A pores (Chiou et al., 1989; Roux and Karplus, 1991; Chiu et al., 1993), which suggests that the nature of the water transport mechanism is intermediate between one-vacancy mediated and continuum processes. Furthermore, x-ray crystallography studies show that hydrophilic cavities in soluble proteins are either saturated with water or have at most one vacancy (see, for instance, the number of solvent sites reported for globular proteins in Hendrickson and Wüthrich, 1991–1994). From all of the above, analytical models of water transport through narrow pores at near-saturation apparently need only consider one-vacancy and full saturation mechanisms.

Both the analytical and numerical studies performed here show only a very small variation of the osmotic permeability coefficient as a function of the water activity in the physiological range. This suggests that water transport through narrow pores exhibits a "Newtonian-like" behavior of the permeability coefficient, characteristic of bulk flow of water in continuous media. It is difficult to predict whether more complicated models representing longer and wider pores would give rise to permeability coefficients that would not obey the "independence principle" in a noticeable fashion.

Another conclusion of this study, illustrated by the examples shown in Fig. 7, is that a particular value of a permeability coefficient can be associated with different numerical values of some of the rate constants. As also shown in the simulations of Fig. 7, such different values could correspond to different regimes of the transport process, which could not be identified by the numerical value of the permeability coefficient by itself.

This work was supported by National Institutes of Health grants EY06178, EY08918, and by Research to Prevent Blindness, Inc. (a Departmental Award, and an International Research Scholarship to J. A. Hernandez).

APPENDIX

Steady-state analysis of the single-file pore model for the case $n = 2$

We perform here the steady-state analysis of the vacancy portion of the model of Fig. 3, using the diagram method developed by Hill (1977). The following symbols represent:

b_e, b_i: rate constants of binding from compartments e and i
r_e, r_i: rate constants of release to compartments e and i
k_{12}, k_{21}: rate constants of forward and backward transitions between positions 1 and 2
N: total number of pores per unit area
w_e, w_i: activities of w in compartments e and i

The flux of w, taken positive in the e to i direction, is given by

$$J_w = J_1 - J_2, \tag{A1}$$

where J_1 and J_2 are the cycle fluxes corresponding to cycles 1 and 2, respectively (Fig. 3 *B*), taken positive in the clockwise direction. From (A1), we express J_w by

$$J_w = \left(\frac{N\pi}{\sum}\right)\left(\sum_1 + \sum_2\right)(w_e - w_i), \tag{A2}$$

where, from the detailed balance restriction,

$$\pi = b_e k_{12} r_i = b_i k_{21} r_e. \tag{A3}$$

The terms $\sum_1$ and $\sum_2$ are the sums of the appendages to cycles 1 and 2, respectively, and are given by

$$\sum_1 = r_e + r_i; \qquad \sum_2 = b_e w_e + b_i w_i. \tag{A4}$$

The denominator $\sum$ is the sum of all the directional diagrams of all the states of the model and is given by

$$\begin{aligned}\sum = {} & (b_e w_e + b_i w_i + r_e + r_i) \times (r_e r_i + b_e w_e r_i + b_i w_i r_e + b_e w_e b_i w_i) \\ & + (k_{12} b_e w_e + k_{21} b_i w_i)(b_e w_e + b_i w_i) + (k_{12} r_i + k_{21} r_e)(r_e + r_i) \\ & + (b_e w_e + b_i w_i)(r_e + r_i)(k_{12} + k_{21}).\end{aligned} \tag{A5}$$

The net fluxes determined by each of the cycles 1 and 2 functioning separately are given by

$$(J_w)_1 = (N\pi/\Omega_1)(w_e - w_i), \tag{A6}$$

and

$$(J_w)_2 = (N\pi/\Omega_2)(w_e - w_i), \tag{A7}$$

where Ω_1 and Ω_2 are the sums of all the directional diagrams of all the states belonging to cycle 1 and cycle 2, respectively, and are given by

$$\begin{aligned}\Omega_1 = {} & r_e r_i + r_e (k_{21} + b_i w_i) + r_i (k_{12} + b_e w_e) \\ & + (k_{12} + k_{21})(b_e w_e + b_i w_i),\end{aligned} \tag{A8}$$

and

$$\begin{aligned}\Omega_2 = {} & b_e w_e b_i w_i + b_e w_e (k_{12} + r_i) + b_i w_i (k_{21} + r_e) \\ & + (k_{12} + k_{21})(r_e + r_i).\end{aligned} \tag{A9}$$

From Eqs. A6 and A7, the permeability coefficients characterizing the transport of w by cycles 1 and 2 functioning separately are, respectively,

$$(P_w)_1 = (N\pi/\Omega_1), \tag{A10}$$

and

$$(P_w)_2 = (N\pi/\Omega_2). \tag{A11}$$

REFERENCES

Chiu, S. W., J. A. Novotny, and E. Jakobsson. 1993. The nature of ion and barrier crossings in a simulated ion channel. *Biophys. J.* 64:98–108.

Chiu, S. W., S. Subramaniam, E. Jakobsson, and J. A. McCammon. 1989. Water and polypeptide conformations in the gramicidin channel. A molecular dynamics study. *Biophys. J.* 56:253–261.

Dani, J. A. 1989. Open channel structure and ion binding sites of the nicotinic acetylcholine receptor channel. *J. Neurosci.* 9:884–892.

Denker, B. M., B. L. Smith, F. P. Kuhajda, and P. Agre. 1988. Identification, purification, and partial characterization of a novel M_r 28,000 integral membrane protein from erythrocytes and renal tubules. *J. Biol. Chem.* 263:15634–15642.

Finkelstein, A. 1987. Water Movement through Lipid Bilayers, Pores and Plasma Membranes: Theory and Reality. John Wiley & Sons, New York.

Finkelstein, A., and P. A. Rosenberg. 1979. Single-file transport: implications for ion and water movement through gramicidin A channels. *In* Membrane Transport Processes. Vol. 3. C. F. Stevens and R. W. Tsien, editors. Raven Press, New York. 73–88.

Fischbarg, J., K. Kuang, J. C. Vera, S. Arant, S. C. Silverstein, J. Loike, and O. M. Rosen. 1990. Glucose transporters serve as water channels. *Proc. Natl. Acad. Sci. USA.* 87:3244–3247.

Hasegawa, H., W. Skach, O. Baker, M. C. Calayag, V. Lingappa, and A. S. Verkman. 1992. A multifunctional aqueous channel formed by CFTR. *Science.* 258:1477–1479.

Heckmann, K. 1965a. Zur theorie der "single file"-diffusion I. *Z. Phys. Chem.* 44:184–203.

Heckmann, K. 1965b. Zur theorie der "single file"-diffusion II. *Z. Phys. Chem.* 46:1–25.

Heckmann, K. 1968. Zur theorie der "single file"-diffusion. III. Sigmoide konzentrationsabhängigkeit unidirektionaler flüsse bei "single file"-diffusion. *Z. Phys. Chem.* 58:201–219.

Hendrickson, W. A., and K. Wüthrich, editors. Macromolecular Structures. Current Biology Ltd., London, 1991.

Hernández, J. A., and J. Fischbarg. 1992. Kinetic analysis of water transport through a single-file pore. *J. Gen. Physiol.* 99:645–662.

Hill, T. L. 1977. Free Energy Transduction in Biology. Academic Press, New York.

Hille, B. 1975. Ionic selectivity, saturation, and block in sodium channels. A four-barrier model. *J. Gen. Physiol.* 66:535–560.

Hille, B. 1992. Ionic Channels of Excitable Membranes, 2nd Edition. Sinauer Associates Inc., Sunderland, MA.

Hodgkin, A. L., and R. D. Keynes. 1955. The potassium permeability of a giant nerve fibre. *J. Physiol.* 128:61–88.

House, C. R. 1974. Water Transport in Cells and Tissues. Williams & Wilkins, Baltimore, MD.

King, E. L., and C. Altman. 1956. A schematic method of deriving the rate laws for enzyme-catalysed reactions. *J. Phys. Chem.* 60:1375–1378.

Kohler, H.-H., and K. Heckmann. 1979. Unidirectional fluxes in saturated single-file pores of biological and artificial membranes. I. Pores containing no more than one vacancy. *J. Theor. Biol.* 79:381–401.

Kohler, H.-H., and K. Heckmann. 1980. Unidirectional fluxes in saturated single-file pores of biological and artificial membranes. II. Asymptotic behavior at high degrees of saturation. *J. Theor. Biol.* 85:575–595.

Levitt, D. G. 1974. A new theory of transport for cell membrane pores. I. General theory and application to red cell. *Biochim. Biophys. Acta.* 373: 115–131.

Levitt, D. G. 1984. Kinetics of movement in narrow channels. *In* Current Topics in Membrane and Transport. Vol. 21. F. Bronner and W. D. Stein, editors. Academic Press, Orlando, FL. 181–197.

Preston, G. M., T. P. Carroll, W. B. Guggino, and P. Agre. 1992. Appearance of water channels in *Xenopus* oocytes expressing red cell CHIP28 protein. *Science.* 256:385–387.

Roux, B., and M. Karplus. 1991. Ion transport in a gramicidin-like channel: dynamics and mobility. *J. Phys. Chem.* 95:4856–4868.

Schultz, S. G. 1980. Basic Principles of Membrane Transport. Cambridge University Press, Cambridge, UK.

Schumaker, M. F., and R. MacKinnon. 1990. A simple model for multi-ion permeation. Single-vacancy conduction in a simple pore model. *Biophys. J.* 58:975–984.

Urban, B. W., and S. B. Hladky. 1979. Ion transport in the simplest single file pore. *Biochim. Biophys. Acta.* 554:410–429.

Urban, B. W., S. B. Hladky, and D. A. Haydon. 1980. Ion movement in gramicidin pores. An example of single-file transport. *Biochim. Biophys. Acta.* 602:331–354.

Verkman, A. S. 1992. Water channels in cell membranes. *Annu. Rev. Physiol.* 54:97–108.

Zhang, R., S. L. Alper, B. Thorens, and A. S. Verkman. 1991. Evidence from oocyte expression that the erythrocyte water channel is distinct from band 3 and the glucose transporter. *J. Clin. Invest.* 88:1553–1558.